Received: 24 March 2017 | Revised: 2 August 2017 | Accepted: 21 August 2017

DOI: 10.1002/num.22201

RESEARCH ARTICLE

WILEY

Supercloseness analysis and polynomial preserving Recovery for a class of weak Galerkin Methods

Ruishu Wang[1] | **Ran Zhang**[1] | **Xu Zhang**[2] | **Zhimin Zhang**[3,4]

[1]School of Mathematics, Jilin University, Changchun 130012, China

[2]Department of Mathematics and Statistics, Mississippi State University, Mississippi State, MS 39762

[3]Beijing Computational Science Research Center, Beijing 100193, China

[4]Department of Mathematics, Wayne State University, Detroit, MI 48202

Correspondence
Xu Zhang, Department of Mathematics and Statistics, Mississippi State University, Mississippi State, MS 39762, USA.
Email: xuzhang@math.msstate.edu

Funding information
The research of this author was supported in part by China Natural National Science Foundation (U1530116, 91630201, 11471141), and by the Program for Cheung Kong Scholars of Ministry of Education of China, Key Laboratory of Symbolic Computation and Knowledge Engineering of Ministry of Education, Jilin University, Changchun, 130012, P.R. China. (R. Z.). The research of this author was supported in part by the National Natural Science Foundation of China grants 11471031, 91430216, U1530401 and the US National Science Foundation grant DMS-1401090 (Z. Z.).

In this article, we analyze convergence and supercloseness properties of a class of weak Galerkin (WG) finite element methods for solving second-order elliptic problems. It is shown that the WG solution is superclose to the Lagrange interpolant using Lobatto points. This supercloseness behavior is obtained through some newly designed stabilization terms. A postprocessing technique using polynomial preserving recovery (PPR) is introduced for the WG approximation. Superconvergence analysis is performed for the PPR recovered gradient. Numerical examples are provided to illustrate our theoretical results.

KEYWORDS
second-order elliptic equation, polynomial preserving recovery, supercloseness, superconvergence, weak Galerkin method

1 | INTRODUCTION

Weak Galerkin (WG) finite element methods (FEM) refer to a new class of finite element discretizations for solving partial differential equations (PDE). In the WG method, classical differential operators are replaced by generalized differential operators as distributions. Unlike the classical FEM that impose continuity in the approximation space, WG methods enforce the continuity weakly in the formulation using generalized weak derivatives and parameter-free stabilizers. WG methods are naturally extended from the standard FEM, and are more advantageous over FEM in several aspects. For instance, high-order WG spaces are usually constructed more conveniently than conforming FEM spaces, as there is no continuity requirement on the approximation spaces. Also, the relaxation of the continuity requirement enables easy implementation of WG methods on polygonal meshes.

The first WG method was introduced in [1] for the second-order elliptic equation, in which the $H(\mathrm{div})$ finite elements such as Raviart-Thomas elements are used to approximate weak gradients. Later in [2, 3], WG methods following the stabilization approach were introduced, which can be applied on polygonal meshes. This new stabilized WG discretization has been applied to many classical PDE models, for example, the biharmonic equation [4, 5].

It is well known that superconvergence/supercloseness is an important and desirable mathematical property of numerical methods for solving PDE. Due to its wide application, superconvergence for standard FEM has been extensively studied in the past decades, see for example [6–12]. The goal of this article is to analyze the supercloseness property of a class of WG methods with generalized stabilizers. Unlike the stabilizer introduced in [2], there is a fine-tune parameter in our new stabilizer (2.4), and it reduces to the standard stabilizer when the parameter $\alpha = 1$. We will show that this new parameter plays a critical role in the analysis for supercloseness. To be more specific, we show that the new WG solutions are superclose to a Lagrange-type interpolant of the exact solution.

Another focus of this article is to develop an efficient postprocessing technique for WG methods which leads to a better approximation of the gradient of the solution. We adopt the polynomial preserving recovery (PPR) technique [13–15] in our postprocessing. The main idea of PPR is to construct a higher-order polynomial locally around each node based on the current numerical solution. Unlike the standard FEM approximation which is a continuous function, the WG solution is discontinuous across the boundary of elements; hence, there can be multiple values associated with a single node. Consequently, we will need to introduce an appropriate weighted average to unify these values before applying the standard PPR scheme. The analysis of superconvergence of PPR scheme relies heavily on the aforementioned supercloseness property.

We note that there are some literature on supercloseness and superconvergence analysis of WG methods. In [1], the supercloseness between the WG solution u_h and the L^2 projection $Q_h u$ is shown. However, there is no discussion about superconvergence behavior between the WG solution u_h and the exact solution u. In [16], superconvergence of the WG solution u_h is shown using the L^2 projection of the WG solution on a coarser mesh but with a higher-order polynomials. In this article, we use PPR recovery to obtain the superconvergence on the same mesh. We note that this is a theoretical work where we show that the recovery techniques work for the WG just as for the standard finite element method. Although our theoretical results are obtained for the Laplace equation on rectangular meshes, the numerical method itself can be applied to other equations and triangular meshes.

The rest of the article is organized as follows. In Section 2, we introduce the definition of weak functions/derivatives, and present the WG method for the model second-order elliptic equation. In Section 3, we describe a Lagrange type interpolation operator which is used in the supercloseness

analysis. In Section 4, we present the error estimation for supercloseness. Section 5 is devoted to the construction of the PPR operator for WG solutions. In Section 6, we present the superconvergence analysis for PPR scheme. In Section 7, we provide some numerical experiments. Brief conclusions are presented in Section 8.

2 | THE WEAK GALERKIN METHOD

In this article, we consider the following second-order elliptic problem with homogeneous Dirichlet boundary condition as a model problem:

$$\begin{aligned} -\Delta u &= f, \quad \text{in } \Omega, \\ u &= 0, \quad \text{on } \partial\Omega, \end{aligned} \tag{2.1}$$

where $\Omega \subset \mathbb{R}^2$ is an open rectangular domain or a finite union of rectangular domains.

The weak formulation for (2.1) can be written as: find $u \in H_0^1(\Omega)$ such that

$$(\nabla u, \nabla v) = (f, v), \quad \forall v \in H_0^1(\Omega), \tag{2.2}$$

where $(\cdot,\cdot)$ is the L^2-inner product, and $H_0^1(\Omega)$ is a subspace of Sobolev space $H^1(\Omega) = \{v : v \in L^2(\Omega), \nabla v \in [L^2(\Omega)]^2\}$ with vanishing boundary value.

Let $\mathcal{T}_h$ be a shape-regular rectangular mesh of domain Ω. For each element $T \in \mathcal{T}_h$, denote by h_T the diameter of T. The mesh size of $\mathcal{T}_h$ is defined as $h = \max_{T\in\mathcal{T}_h} h_T$. Denote by $\mathcal{E}_h$ the set of all edges in $\mathcal{T}_h$ and $\mathcal{E}_h^0 = \mathcal{E}_h \setminus \partial\Omega$ the set of all interior edges in $\mathcal{T}_h$. Let $Q_k(T)$ be a set of polynomials that the degrees of x and y are no more than k, and let

$$Q_k = \{v : v|_T \in Q_k(T), \forall T \in \mathcal{T}_h\}.$$

Define the space of weak functions on every element T by

$$\mathcal{V}(T) = \{v = \{v_0, v_b\} : v_0 \in L^2(T), v_b \in L^2(\partial T)\}.$$

Note that v_0 and v_b are completely independent.

Definition 2.1 ([1]) Denote by $\nabla_w v$ the weak gradient of $v \in \mathcal{V}(T)$ as a linear functional of the Sobolev space $H(div; T) = \{\mathbf{q} \in [L^2(T)]^2 : \nabla \cdot \mathbf{q} \in L^2(T)\}$. That is the action on any function $\mathbf{q} \in H(div; T)$ is given by

$$\langle \nabla_w v, \mathbf{q}\rangle_T := -(v_0, \nabla \cdot \mathbf{q})_T + \langle v_b, \mathbf{q} \cdot \mathbf{n}\rangle_{\partial T},$$

where $\mathbf{n}$ is the unit outward normal vector on ∂T.

Next, we define the space $W_r(T)$ to be

$$W_r(T) = [Q_{r-1,r}, Q_{r,r-1}]^t,$$

where $Q_{i,j}$ is a set of polynomials whose degrees of x and y are no more than i and j, respectively.

Definition 2.2 The discrete weak gradient operator of $v \in \mathcal{V}(T)$, denoted by $\nabla_{w,r,T} v \in W_r(T)$, is the unique function in $W_r(T)$, satisfying

$$(\nabla_{w,r,T} v, \mathbf{q})_T = -(v_0, \nabla \cdot \mathbf{q})_T + \langle v_b, \mathbf{q} \cdot \mathbf{n} \rangle_{\partial T}, \quad \forall \mathbf{q} \in W_r(T), \tag{2.3}$$

where $\mathbf{n}$ is the unit outward normal vector on ∂T.

Let V_h and W_h be the global WG spaces of weak functions and weak gradients as follows

$$V_h = \{v = \{v_0, v_b\} : v_0|_T \in Q_k(T), v_b|_e \in P_k(e), e \subset \partial T, T \in \mathcal{T}_h\},$$
$$W_h = \{\mathbf{q} : \mathbf{q}|_T \in W_k(T), T \in \mathcal{T}_h\}.$$

Note that any weak function v in V_h has a single-valued component v_b on each edge $e \in \mathcal{E}_h$. Let V_h^0 be the subspace of V_h with vanishing boundary value on $\partial\Omega$.

For each $v \in V_h$, the discrete weak gradient $\nabla_{w,k} v \in W_h$ is computed piecewisely using (2.3) on each element $T \in \mathcal{T}_h$, i.e.,

$$(\nabla_{w,k} v)|_T = \nabla_{w,k,T}(v|_T), \quad \forall v \in V_h.$$

For simplicity, we drop the subscript k from the notation $\nabla_{w,k}$ in the rest of the article.

Define the following bilinear forms

$$s(w, v) = \sum_{T \in \mathcal{T}_h} h^{-\alpha} \langle w_0 - w_b, v_0 - v_b \rangle_{\partial T}, \quad \alpha \geq 1, \forall w, v \in V_h, \tag{2.4}$$

$$a_s(w, v) = (\nabla_w w, \nabla_w v)_h + s(w, v), \quad \forall w, v \in V_h, \tag{2.5}$$

where $(\cdot, \cdot)_h = \sum_{T \in \mathcal{T}_h} (\cdot, \cdot)_T$.

Lemma 2.3 *The functional $|||\cdot||| : V_h \to \mathbb{R}$ defined by*

$$|||v|||^2 = a_s(v, v), \quad \forall v \in V_h, \tag{2.6}$$

is a norm on the space V_h^0. Moreover,

$$\sum_{T \in \mathcal{T}_h} \|\nabla v_0\|_T^2 \leq C|||v|||^2, \quad \forall v \in V_h, \tag{2.7}$$

$$\sum_{T \in \mathcal{T}_h} h_T^{-1} \|v_0 - v_b\|_{\partial T}^2 \leq C|||v|||^2, \quad \forall v \in V_h. \tag{2.8}$$

Proof It is easy to see that $|||\cdot|||$ is a semi-norm in V_h^0. Hence, it suffices to show that $v = 0$ whenever $|||v||| = 0$. Using (2.4) and (2.5), we have

$$0 = |||v|||^2 = a_s(v, v) = (\nabla_w v, \nabla_w v)_h + \sum_{T \in \mathcal{T}_h} h^{-\alpha} \langle v_0 - v_b, v_0 - v_b \rangle_{\partial T}.$$

That is $\nabla_w v = 0$ on each $T \in \mathcal{T}_h$, and $v_0|_e = v_b$ on each $e \in \mathcal{E}_h$. It follows from $v_0|_e = v_b$ that

$$\begin{aligned} 0 &= (\nabla_w v, \mathbf{q})_T = -(v_0, \nabla \cdot \mathbf{q})_T + \langle v_b, \mathbf{q} \cdot \mathbf{n} \rangle_{\partial T} \\ &= (\nabla v_0, \mathbf{q})_T - \langle v_0 - v_b, \mathbf{q} \cdot \mathbf{n} \rangle_{\partial T} = (\nabla v_0, \mathbf{q})_T, \quad \forall \mathbf{q} \in W_k(T), \end{aligned} \tag{2.9}$$

where $\mathbf{n}$ is the outward normal of ∂T. Thus $\nabla v_0 = 0$ on each $T \in \mathcal{T}_h$, and v_0 is a constant on each T. Together with $v_0|_e = v_b$, we conclude that v is a constant on the global domain Ω. The fact $v \in V_h^0$ implies $v = 0$. As a result, $|||\cdot|||$ is a norm in space V_h^0.

For any $v = \{v_0, v_b\} \in V_h$, it follows from the definition of weak gradient, the trace inequality, the inverse inequality, and the assumption $\alpha \geq 1$ that

$$\begin{aligned} \sum_{T \in \mathcal{T}_h} \|\nabla v_0\|_T^2 &= \sum_{T \in \mathcal{T}_h} (\nabla v_0, \nabla v_0)_T \\ &= \sum_{T \in \mathcal{T}_h} (\nabla_w v, \nabla v_0)_T + \sum_{T \in \mathcal{T}_h} \langle v_0 - v_b, \nabla v_0 \cdot \mathbf{n} \rangle_{\partial T} \\ &\leq \left(\sum_{T \in \mathcal{T}_h} \|\nabla_w v\|_T^2 \right)^{\frac{1}{2}} \left(\sum_{T \in \mathcal{T}_h} \|\nabla v_0\|_T^2 \right)^{\frac{1}{2}} \\ &\quad + \left(\sum_{T \in \mathcal{T}_h} h_T^{-\alpha} \|v_0 - v_b\|_{\partial T}^2 \right)^{\frac{1}{2}} \left(\sum_{T \in \mathcal{T}_h} h^{\alpha} \|\nabla v_0\|_{\partial T}^2 \right)^{\frac{1}{2}} \\ &\leq C |||v||| \left(\sum_{T \in \mathcal{T}_h} \|\nabla v_0\|_T^2 \right)^{\frac{1}{2}}. \end{aligned}$$

We obtain (2.7). The inequality (2.8) follows from that h is small and $\alpha \geq 1$. ∎

We consider the following weak Galerkin method: find $u_h \in V_h^0$ such that

$$a_s(u_h, v) = (f, v_0), \quad \forall v \in V_h^0, \tag{2.10}$$

where $(f, v_0) = \sum_{T \in \mathcal{T}_h} (f, v_0)_T$.

Remark 2.1 The difference between the WG method (2.10) and the classical WG method in [2] is that the stabilizer contains a fine-tune parameter α. Later on, it will be shown that the parameter α plays an important role in the supercloseness analysis in Section 4. Numerical experiments in Section 7 also demonstrate this feature.

3 | INTERPOLATION OPERATOR

This section introduces an interpolation operator that will be used later in the superconvergence analysis.

Let $-1 = \zeta_0 < \zeta_1 < \cdots < \zeta_k = 1$ be $k+1$ Lobatto points on the reference interval $\hat{e} = [-1, 1]$, which are $k+1$ zeros of the Lobatto polynomial ω_{k+1}. We define a Lagrange interpolation operator $\mathcal{I} : C^0(\hat{e}) \to P_k(\hat{e})$ such that

$$\mathcal{I}u(x) = \sum_{i=0}^{k} u(\zeta_i) l_i(x), \quad u \in C^0(\hat{e}), \tag{3.1}$$

where $l_i, i = 0, 1, \cdots, k$, are the Lagrange interpolation associated with Lobatto points ζ_i. The following properties of l_i can be easily verified:

$$l_i(\zeta_j) = \delta_{ij}, \quad i,j = 0, 1, \ldots, k, \tag{3.2}$$

$$\sum_{i=0}^{k} l_i(x) = 1, \quad \forall x \in \hat{e}, \tag{3.3}$$

$$\sum_{i=0}^{k} (\zeta_i - x)^m l_i(x) = 0, \quad 1 \le m \le k. \tag{3.4}$$

We recall an interpolation error representation in [17].

Lemma 3.1 *Let $u \in H^{k+2}(\hat{e})$. Then we have the following error equation*

$$u(x) - \mathcal{I}u(x) = C\omega_{k+1}(x) u^{(k+1)}(x) + R(u, x),$$

where C is a constant, ω_{k+1} is the Lobatto polynomial with order $k+1$, and

$$R(u, x) = \sum_{i=0}^{k} l_i(x) \int_{\zeta_i}^{x} \frac{(\zeta_i - t)^{k+1}}{(k+1)!} u^{(k+2)}(t) dt.$$

As shown in Lemma 3.1, the interpolation operator $\mathcal{I}$ preserves polynomials of degree up to k. We composite the interpolation operators (3.1) in x- and y-directions to obtain an interpolation operator in the two-dimensional domain $\mathcal{I}_h : C^0(\Omega) \to \mathcal{S}_h := Q_k \cap C^0(\Omega)$ such that

$$(\mathcal{I}_h u)|_T = \mathcal{I}_1 \mathcal{I}_2 u|_T = \mathcal{I}_1 \left(\sum_{i=0}^{k} u(x, \zeta_i^2) l_i(y) \right) = \sum_{j=0}^{k} \sum_{i=0}^{k} u(\zeta_j^1, \zeta_i^2) l_i(y) l_j(x), \tag{3.5}$$

where $\mathcal{I}_1, \mathcal{I}_2$ are the interpolation operators in x-, y-directions, respectively. From (3.5), it is easy to prove $\mathcal{I}_h u \in C^0(\Omega)$. By Lemma 3.1, we have the following estimates.

Lemma 3.2 ([17]) *There exists a constant C such that for any $u \in H^{k+2}(T)$, the following inequality holds true*

$$(\nabla(u - \mathcal{I}_h u), \nabla v)_T \le C h^{k+1} |u|_{k+2,T} |v|_{1,T}, \quad \forall v \in Q_k(T). \tag{3.6}$$

The definition of ∇_w in (2.3) and the fact that $\mathcal{I}_h v \in C^0$ yield the following lemma.

Lemma 3.3 *The interpolation operator defined in (3.5) satisfies*

$$(\nabla_w \mathcal{I}_h v, \mathbf{q})_h = (\nabla \mathcal{I}_h v, \mathbf{q})_h, \quad \forall v \in C^0(\Omega), \mathbf{q} \in W_h, \tag{3.7}$$

where $(\cdot, \cdot)_h = \sum_{T \in \mathcal{T}_h} (\cdot, \cdot)_T$.

4 | ANALYSIS OF SUPERCLOSENESS

In this section, we derive an error estimate for $|||\mathcal{I}_h u - u_h|||$, where u_h is the solution of the WG method (2.10) and $\mathcal{I}_h u$ is the interpolation of the exact solution of problem (2.1).

Theorem 4.1 *Let $u \in H^{k+2}(\Omega)$ be the solution of (2.1), and $u_h \in V_h$ be the solution of WG method (2.10). The following error estimate holds*

$$|||\mathcal{I}_h u - u_h||| \leq C h^{\min\left\{k+1, k+\frac{\alpha-1}{2}\right\}} \|u\|_{k+2}. \tag{4.1}$$

Proof As $Q_k \subset V_h$, then $|||\mathcal{I}_h u - u_h|||$ is well-defined. Multiplying both sides of (2.1) by v_0, and using integration by parts, we have

$$\begin{aligned}(f, v_0) &= \sum_{T\in\mathcal{T}_h} (-\Delta u, v_0)_T = \sum_{T\in\mathcal{T}_h} (\nabla u, \nabla v_0)_T - \sum_{T\in\mathcal{T}_h} \langle \nabla u \cdot \mathbf{n}, v_0\rangle_{\partial T} \\ &= \sum_{T\in\mathcal{T}_h} (\nabla u, \nabla v_0)_T - \sum_{T\in\mathcal{T}_h} \langle \nabla u \cdot \mathbf{n}, v_0 - v_b\rangle_{\partial T}. \end{aligned} \tag{4.2}$$

Here, we use the facts that the normal component $\nabla u \cdot \mathbf{n}$ of the flux is continuous on all interior edges and $v_b|_{\partial\Omega} = 0$.

From (2.10), (3.7), (4.2), the Cauchy-Schwarz inequality, (3.6), (2.7), the property of interpolation operator $\mathcal{I}_h$, and $\alpha \geq 1$ we obtain

$$\begin{aligned}|||\mathcal{I}_h u - u_h|||^2 &= a_s(\mathcal{I}_h u - u_h, \mathcal{I}_h u - u_h) \\ &= a_s(\mathcal{I}_h u, \mathcal{I}_h u - u_h) - a_s(u_h, \mathcal{I}_h u - u_h) \\ &= \sum_{T\in\mathcal{T}_h} (\nabla_w \mathcal{I}_h u, \nabla_w(\mathcal{I}_h u - u_h))_T - (f, \mathcal{I}_h u - u_0) \\ &= \sum_{T\in\mathcal{T}_h} (\nabla \mathcal{I}_h u, \nabla_w(\mathcal{I}_h u - u_h))_T - \sum_{T\in\mathcal{T}_h} (\nabla u, \nabla(\mathcal{I}_h u - u_0))_T \\ &\quad + \sum_{T\in\mathcal{T}_h} \langle \nabla u \cdot \mathbf{n}, \mathcal{I}_h u - u_0 - (\mathcal{I}_h u - u_b)\rangle_{\partial T} \\ &= \sum_{T\in\mathcal{T}_h} (\nabla(\mathcal{I}_h u - u), \nabla(\mathcal{I}_h u - u_0))_T \\ &\quad - \sum_{T\in\mathcal{T}_h} \langle \nabla(\mathcal{I}_h u - u) \cdot \mathbf{n}, \mathcal{I}_h u - u_0 - (\mathcal{I}_h u - u_b)\rangle_{\partial T} \\ &\leq \sum_{T\in\mathcal{T}_h} (\nabla(\mathcal{I}_h u - u), \nabla(\mathcal{I}_h u - u_0))_T \\ &\quad + \left(\sum_{T\in\mathcal{T}_h} h_T^{\alpha} \|\nabla(\mathcal{I}_h u - u)\|_{\partial T}^2\right)^{\frac{1}{2}} \left(\sum_{T\in\mathcal{T}_h} h_T^{-\alpha} \|\mathcal{I}_h u - u_0 - (\mathcal{I}_h u - u_b)\|_{\partial T}^2\right)^{\frac{1}{2}} \\ &\leq C h^{\min\left\{k+1, k+\frac{\alpha-1}{2}\right\}} \|u\|_{k+2} |||\mathcal{I}_h u - u_h|||. \end{aligned}$$

Here, we have used the fact that $\nabla(\mathcal{I}_h u) \in W_h$. ∎

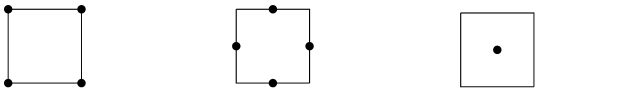

(a) Vertex (b) Edge node (c) Internal node

FIGURE 1 Three types of nodes. (a) Vertex. (b) Edge node. (c) Internal node

Remark 4.1 The estimate (4.1) shows that the WG solution u_h is superclose to the interpolation $\mathcal{I}_h u$ when $\alpha > 1$. It reaches the maximum rate of convergence when $\alpha = 3$. Further increasing the value of α will not improve the rate of convergence.

5 | PPR FOR WG SOLUTIONS

In this section, we introduce a gradient recovery operator G_h onto space $S_h \times S_h$, with $S_h := \{v \in C^0(\Omega) : v|_T \in P_k(T), T \in \mathcal{T}_h\}$, on the rectangular mesh $\mathcal{T}_h$. For a WG solution u_h in (2.10), we define $G_h u_h$ on the following three types of mesh nodes [15]: vertex, edge node, and internal node, see Figure 1.

5.1 | Vertex patch

We define a patch K_z for every vertex z by

$$K_z = \{T \in \mathcal{T}_h : \bar{T} \cap \{z\} \neq \emptyset\}$$

be the union of the elements in the first layer around z. There can be two types of vertices. The first type is the interior vertex $z \in \Omega$, and the other one is the boundary vertex $z \in \partial\Omega$, see Figure 2 for an illustration.

Before we introduce the PPR scheme, we need to clarify some notations.

- $\mathcal{N}$: All nodes in $\overline{\Omega}$. They could be vertices, edge nodes, or internal nodes.
- $\mathcal{N}(T)$: All mesh nodes in $\bar{T}$.
- $\mathcal{N}_i$: $\mathcal{N}_i = \{z_{i,j}\}_{j=1}^{n_{z_i}}$ is the set of all mesh nodes in $\overline{K_{z_i}}$. Here, n_{z_i} is the number of the nodes. For the bilinear element, all nodes are vertices. For quadratic and higher-order elements, there are vertices, edge nodes, and internal nodes.
- $\mathcal{M}^0$: All interior vertices in Ω.

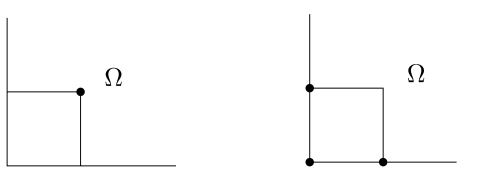

(a) Interior vertex (b) Boundary vertex

FIGURE 2 Two kinds of vertices. (a) Interior vertex. (b) Boundary vertex

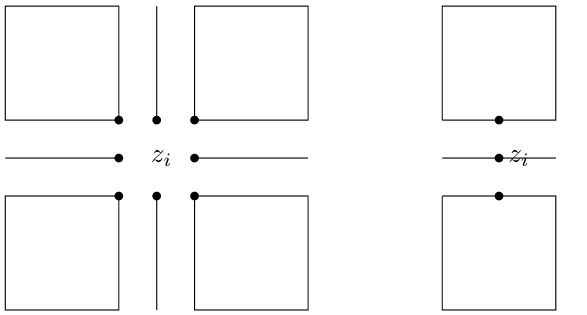

(a) Interior vertex (b) Edge node

FIGURE 3 The distribution of u_h on a mesh node z_i. (a) Interior vertex. (b) Edge node

- $\mathcal{M}^0(T)$: All interior vertices in $\bar{T} \cap \Omega$.
- $\mathcal{M}_i^0 : \mathcal{M}_i^0 = \{z_{i,j}\}_{j=1}^{m_{z_i}}$ is the set of all interior vertices in $\overline{K_{z_i}}$. Denoted by m_{z_i} the number of nodes in $\mathcal{M}_i^0$.

5.2 | The reformulated value $\bar{u}_h$

To obtain the recovered gradient $G_h u_h(z_i)$, we need to use the values of u_h at mesh nodes in $\mathcal{N}_i$ to get an approximation $p_{k+1} \in P_{k+1}(K_{z_i})$ in the least-square sense. However, on a vertex or an edge node, the WG solution u_h may have more than one value, as illustrated in Figure 3. As a result, we must redefine the value of u_h at those nodes.

For any node $z_i \in \mathcal{N}$, denote by $\{u_h^j(z_i)\}_{j=1}^{l_{z_i}}$ the possible values for u_h at z_i where l_{z_i} is the number of these values. Note that $u_h^j(z_i)$ might be the value of the interior part u_0 or the boundary part u_b of the weak function $u_h = \{u_0, u_b\}$ at point z_i. We define a function $\bar{u}_h$ such that the value of $\bar{u}_h$ at z_i is given by

$$\bar{u}_h(z_i) = \sum_{j=1}^{l_{z_i}} \alpha_j u_h^j(z_i), \quad \alpha_j \geq 0, \quad \sum_{j=1}^{l_{z_i}} \alpha_j = 1. \tag{5.1}$$

Moreover, we require $\bar{u}_h \in \mathcal{S}_h$ to be a function satisfying

$$\bar{u}_h = \sum_{z_i \in \mathcal{N}} \bar{u}_h(z_i) l_i, \tag{5.2}$$

where l_i is the Lagrange basis associated with z_i. It can be proved that the function $\bar{u}_h$ satisfies the following lemma.

Lemma 5.1 *Given $u_h = \{u_0, u_b\} \in V_h$, let $\bar{u}_h$ be defined as (5.1)–(5.2). Assume that $z_i \in \mathcal{M}^0$ is an interior vertex, K_{z_i} is the patch for z_i, and $\mathcal{N}_i = \{z_{i,j}\}_{j=1}^{n_{z_i}}$ is the set of the nodes in $\overline{K_{z_i}}$, where n_{z_i} is the number of the elements in $\mathcal{N}_i$. Then for $T \subset K_{z_i}$, $z_{i,j} \in \bar{T}$, the following properties hold.*

(i) $(\bar{u}_h - u_0)|_T(z_{i,j})$ *can be written as the jump of u_h at $z_{i,j}$, if $z_{i,j} \in \mathcal{N}_i$ is a vertex or an edge node on ∂T,*

(ii) $(\bar{u}_h - u_0)|_T(z_{i,j}) = 0$, *if $z_{i,j} \in \mathcal{N}_i$ is an internal mesh node in T.*

Proof Without loss of generality, we consider an interior vertex $z_{i,1}$. Assume that $u_0^1, \ldots, u_0^4$, $u_b^5, \ldots, u_b^8$ are the values of u_h at $z_{i,1}$, see the left plot in Figure 3. Let $\bar{u}_h(z_{i,1}) = \sum_{s=1}^{4} \alpha_s u_0^s + \sum_{t=5}^{8} \alpha_t u_b^t$ and $u_0|_T(z_{i,1}) = u_0^1$. Then, we have

$$(\bar{u}_h - u_0)|_T(z_{i,1}) = \sum_{s=1}^{4} \alpha_s (u_0^s - u_0^1) + \sum_{t=5}^{8} \alpha_t (u_b^t - u_0^1).$$

This shows that $(\bar{u}_h - u_0)|_T(z_{i,1})$ consists of the jump of u_h at $z_{i,1}$. Furthermore, it can be written as $u_0|_e(z_{i,1}) - u_b|_e(z_{i,1})$, where u_0 and u_b share the edge e and $z_{i,1}$ lies on the edge e.

For boundary vertices and edge nodes, the proof is similar. For internal nodes, the property (ii) follows directly from the definition of $\bar{u}_h$. ∎

5.3 | The PPR operator G_h

Recall that the function $\bar{u}_h$ is defined to have a unique value at each node. Therefore, we can apply PPR scheme to construct the gradient recovery operator G_h. We consider the following four cases.

Case 1 For each interior vertex $z_i \in \mathcal{M}^0$, we fit a polynomial in $P_{k+1}(K_{z_i})$ to the redefined WG solution $\bar{u}_h(z_{i,j}), j = 1, \ldots, n_{z_i}$ by the least-square method. Let (x, y) be the local coordinates with respect to the origin z_i. The fitting polynomial is defined as

$$p_{k+1}(x, y; z_i) = \mathbf{P}\mathbf{a} = \hat{\mathbf{P}}\hat{\mathbf{a}}, \tag{5.3}$$

where

$$\begin{aligned}
&\mathbf{P} = (1, x, y, \ldots, x^{k+1}, x^k y, \ldots, y^{k+1}),\\
&\hat{\mathbf{P}} = (1, \hat{x}, \hat{y}, \ldots, \hat{x}^{k+1}, \hat{x}^k \hat{y}, \ldots, \hat{y}^{k+1}),\\
&\mathbf{a} = (a_1, a_2, \ldots, a_m)^t, \quad \hat{\mathbf{a}} = (a_1, h a_2, \ldots, h^{k+1} a_m)^t,
\end{aligned}$$

with $\hat{x} = x/h$ and $\hat{y} = y/h$, and $m = (k+2)(k+3)/2$ is the number of the basis of $P_{k+1}(K_{z_i})$. By the least-square method, the vector $\hat{\mathbf{a}}$ can be solved from

$$A^t A \hat{\mathbf{a}} = A^t \mathbf{b}_h, \tag{5.4}$$

where $\mathbf{b}_h = (\bar{u}_h(z_{i,1}), \bar{u}_h(z_{i,2}), \ldots, \bar{u}_h(z_{i,n_{z_i}}))^t$ and

$$A = \begin{pmatrix}
1 & \hat{x}_1 & \hat{y}_1 & \ldots & \hat{x}_1^{k+1} & \hat{x}_1^k \hat{y}_1 & \ldots & \hat{y}_1^{k+1} \\
1 & \hat{x}_2 & \hat{y}_2 & \ldots & \hat{x}_2^{k+1} & \hat{x}_2^k \hat{y}_2 & \ldots & \hat{y}_2^{k+1} \\
\vdots & \vdots & \vdots & \vdots & \vdots & \vdots & \vdots & \vdots \\
1 & \hat{x}_{n_{z_i}} & \hat{y}_{n_{z_i}} & \ldots & \hat{x}_{n_{z_i}}^{k+1} & \hat{x}_{n_{z_i}}^k \hat{y}_{n_{z_i}} & \ldots & \hat{y}_{n_{z_i}}^{k+1}
\end{pmatrix}$$

where $(\hat{x}_j, \hat{y}_j)$ is the coordinates of $z_{i,j}$ in the reference domain. Define $G_h u_h$ at the point z_i as

$$G_h u_h(z_i) = \nabla p_{k+1}(0, 0; z_i).$$

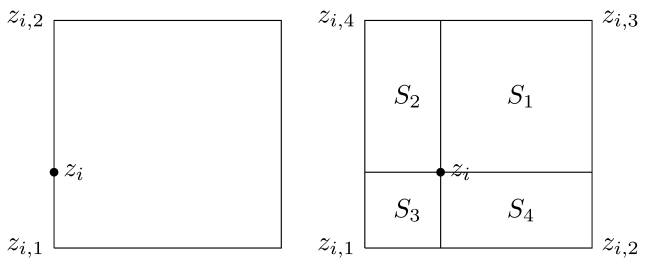

(a) Edge node (b) Internal node

FIGURE 4 The lengths/areas that distributed by node z_i. (a) Edge node. (b) Internal node

Case 2 For a boundary vertex $z_i \in \partial\Omega$, we define

$$G_h u_h(z_i) = \frac{\sum_{z_{i,j} \in \mathcal{M}_i^0} \nabla p_{k+1}(x_j, y_j; z_{i,j})}{m_{z_i}},$$

where m_{z_i} is the number of interior vertices in $\mathcal{M}_i^0$ and (x_j, y_j) is the local coordinates of z_i with $z_{i,j}$ be the origin.

Case 3 For an edge node z_i which lies on an edge between vertices $z_{i,1}$ and $z_{i,2}$, we define

$$G_h u_h(z_i) = \alpha \nabla p_{k+1}(x_1, y_1; z_{i,1}) + (1-\alpha)\nabla p_{k+1}(x_2, y_2; z_{i,2}), \quad 0 \le \alpha \le 1,$$

where (x_1, y_1) and (x_2, y_2) are the coordinates of z_i with respect to the origins $z_{i,1}$ and $z_{i,2}$, respectively. The weight α is determined by the ratio of the distances of z_i to $z_{i,1}$ and $z_{i,2}$, that is $\alpha = |z_i - z_{i,2}|/|z_{i,1} - z_{i,2}|$, see Figure 4a.

Case 4 For an internal node z_i which lies in an element formed by vertices $z_{i,1}$, $z_{i,2}$, $z_{i,3}$, $z_{i,4}$, we define

$$G_h u_h(z_i) = \sum_{j=1}^{4} \alpha_j \nabla p_{k+1}(x_j, y_j; z_{i,j}), \quad \sum_{j=1}^{4} \alpha_j = 1, \alpha_j \ge 0,$$

where (x_j, y_j) is the local coordinates of z_i with respect to the origin $z_{i,j}$. The weight α_j is determined by the space ratio of the opposite patch to $z_{i,j}$, that is $\alpha_j = |S_j|/S$, and $S = \sum_{l=1}^{4} |S_l|$, see Figure 4b.

Remark 5.1 For any $u_h \in V_h$, $G_h u_h$ is defined as the linear combination of the values of $G_h u_h$ at the interior vertex. For $u \in C^0(\Omega)$, we define G_{hu} by

$$G_h u = G_h \mathcal{I}_h u, \tag{5.5}$$

where $\mathcal{I}_h : C^0(\Omega) \to \mathcal{S}_h \subset V_h$ is the interpolation operator given in (3.5).

6 | SUPERCONVERGENCE ESTIMATES

In this section, we report several properties of the operator G_h, and analyze the superconvergence between ∇u and $G_h u_h$.

The following lemma can be directly verified along the same procedure as Lemma 3.10in [14].

Lemma 6.1 *Let $z_i \in \mathcal{M}^0$ be an interior vertex with the patch K_{z_i}, and let $p_{k+1}(\cdot,\cdot;z_i)$ be the least square polynomial of the function $v \in \mathcal{S}_h$ in the patch K_{z_i}. Then there is a constant C such that*

$$|\nabla p_{k+1}(\cdot,\cdot;z_i)|_{\infty,K_{z_i}} \leq Ch^{-1}|v|_{1,K_{z_i}}.$$

By the definition given in Subsection 5.3, G_h is a polynomial-preserving operator which satisfies the following lemma.

Lemma 6.2 *The gradient recovery operator G_h satisfies*

$$G_h u_h = G_h \bar{u}_h, \quad \forall u_h \in V_h, \tag{6.1}$$

$$\|\nabla u - G_h u\| \leq Ch^{k+1}|u|_{k+2}, \quad \forall u \in H^{k+2}(\Omega), \tag{6.2}$$

where C is a constant and $\bar{u}_h \in \mathcal{S}_h$ satisfying (5.1)–(5.2) is the redefined function of u_h.

The next lemma provides an important tool in establishing our main result.

Lemma 6.3 *For $u_h \in V_h$, we have the property that*

$$|||u_h|||^2 \geq \|G_h \bar{u}_h\|^2, \tag{6.3}$$

where $\bar{u}_h \in \mathcal{S}_h$ satisfying (5.1)–(5.2) is the redefined function of u_h.

Proof We will prove (6.3) in three steps.

Step 1. For any $T \in \mathcal{T}_h$, recall that $\mathcal{M}^0(T)$ denotes the set of the interior vertices in $\bar{T} \cap \Omega$. Then, from the definition of G_h, we have

$$\|G_h \bar{u}_h\|_{0,T} \leq C|T|^{\frac{1}{2}} \|G_h \bar{u}_h\|_{\infty,T} \leq C|T|^{\frac{1}{2}} \max_{z_i \in \mathcal{M}^0(T)} \{|\nabla p_{k+1}(\cdot,\cdot;z_i)|_{\infty,K_{z_i}}\}.$$

Using Lemma 6.1, we have

$$\|G_h \bar{u}_h\|_{0,T} \leq C|T|^{\frac{1}{2}} \max_{z_i \in \mathcal{M}^0(T)} \{h^{-1}|\bar{u}_h|_{1,K_{z_i}}\} \leq C \max_{z_i \in \mathcal{M}^0(T)} \{|\bar{u}_h|_{1,K_{z_i}}\}.$$

It follows that

$$\|G_h \bar{u}_h\|^2 = \sum_{T \in \mathcal{T}_h} \|G_h \bar{u}_h\|_{0,T}^2 \leq C \sum_{z_i \in \mathcal{M}^0} |\bar{u}_h|_{1,K_{z_i}}^2. \tag{6.4}$$

Step 2. Define the auxiliary function $\tilde{u}_h$ as

$$\tilde{u}_h = \bar{u}_h - u_0.$$

For any interior vertex $z_i \in \mathcal{M}^0$, it follows from the definition of $\bar{u}_h$ and u_0 that $\tilde{u}_h$ is a piecewise polynomial on K_{z_i}. Then from the triangle inequality we have

$$|\bar{u}_h|^2_{1,K_{z_i}} = |\tilde{u}_h + u_0|^2_{1,K_{z_i}} \leq |\tilde{u}_h|^2_{1,K_{z_i}} + |u_0|^2_{1,K_{z_i}}.$$

It follows from (2.7) that

$$\sum_{z_i \in \mathcal{M}^0} |\bar{u}_h|^2_{1,K_{z_i}} \leq \sum_{z_i \in \mathcal{M}^0} (|\tilde{u}_h|^2_{1,K_{z_i}} + |u_0|^2_{1,K_{z_i}}) \leq C \left(\sum_{z_i \in \mathcal{M}^0} |\tilde{u}_h|^2_{1,K_{z_i}} + |||u_h|||^2 \right). \tag{6.5}$$

Step 3. We shall prove

$$|\tilde{u}_h|^2_{1,K_{z_i}} \leq C|||u_h|||^2_{K_{z_i}}. \tag{6.6}$$

First, we consider an element $T_1 \subset K_{z_i}$. Let $\tilde{u}_h|_{T_1} = \sum_{z_{i,j} \in \mathcal{N}(T_1)} \tilde{u}_h(z_{i,j}) l_{i,j}$, where $l_{i,j}(z_{k,l}) = \delta_{i,k}\delta_{j,l}$ are the Lagrange bases. Let $\hat{l}_{i,j}$ be the affine function for $l_{i,j}$ on the reference domain. As $|\nabla \hat{l}_{i,j}|$ is uniformly bounded, we obtain

$$\begin{aligned} |\tilde{u}_h|^2_{1,T_1} &= \int_{T_1} |\nabla \tilde{u}_h|^2 dx = \int_{T_1} \left| \nabla \left(\sum_{z_{i,j} \in \mathcal{N}(T_1)} \tilde{u}_h(z_{i,j}) l_{i,j} \right) \right|^2 dx \\ &\leq C \sum_{z_{i,j} \in \mathcal{N}(T_1)} |\tilde{u}_h(z_{i,j})|^2 \int_{\hat{T}_1} |\nabla \hat{l}_{i,j}|^2 d\hat{x} \leq C \sum_{z_{i,j} \in \mathcal{N}(T_1)} |\tilde{u}_h(z_{i,j})|^2. \end{aligned}$$

Let $\mathcal{E}(T_1) = \{e \in \mathcal{E}_h : e \cap \mathcal{N}(T_1) \neq \emptyset\}$ and $[u_h]_e$ be the jump of u_h over e. From Lemma 5.1, we know that the values of $\tilde{u}_h$ on the mesh nodes on ∂T_1 is the combination of the jump of u_h on edges $e \in \mathcal{E}(T_1)$, the values of $\tilde{u}_h$ on the internal mesh nodes in T_1 are zeros. Using the inverse inequality $\|v\|_{\infty,e} \leq Ch^{-\frac{1}{2}}\|v\|_{0,e}$ and (2.8), we obtain

$$\begin{aligned} \sum_{z_{i,j} \in \mathcal{N}(T_1)} |\tilde{u}_h(z_{i,j})|^2 &\leq C \sum_{e \in \mathcal{E}(T_1)} |[u_h]_e|^2_{\infty,e} \leq C \sum_{e \in \mathcal{E}(T_1)} h^{-1} |[u_h]_e|^2_{0,e} \\ &\leq C \sum_{T \in \mathcal{T}_h(T_1)} h^{-1} \langle u_0 - u_b, u_0 - u_b \rangle_{\partial T} \leq C \sum_{T \in \mathcal{T}_h(T_1)} |||u_h|||^2_T, \end{aligned}$$

where $\mathcal{T}_h(T_1) := \{T \in \mathcal{T}_h : T \cap e \neq \emptyset, e \in \mathcal{E}(T_1)\}$. For other three elements $T \in K_{z_i}$, the proof can be finished similarly. Finally, combining (6.4), (6.5), and (6.6), we have

$$\|G_h \bar{u}_h\|^2 \leq C \sum_{z_i \in \mathcal{M}^0} |\bar{u}_h|^2_{1,K_{z_i}} \leq C \left(\sum_{z_i \in \mathcal{M}^0} |\tilde{u}_h|^2_{1,K_{z_i}} + |||u_h|||^2 \right) \leq C|||u_h|||^2. \quad \blacksquare$$

Now we are ready to state our main result for superconvergence.

Theorem 6.4 *Let $u \in H^{k+2}(\Omega)$ be the solution of (2.1) and $u_h \in V_h$ be the solution of (2.10). Let $G_h u_h$ be the recovered gradient by PPR introduced in Section 5.3. Then we have the following error estimate*

$$\|G_h u_h - \nabla u\| \leq C h^{\min\left\{k+1, k+\frac{\alpha-1}{2}\right\}} \|u\|_{k+2}. \tag{6.7}$$

Proof It follows from (6.1), (5.5), (6.2), (6.3), and (4.1) that

$$\begin{aligned}
\|G_h u_h - \nabla u\|^2 &\leq \|G_h u_h - G_h \mathcal{I}_h u\|^2 + \|G_h \mathcal{I}_h u - \nabla u\|^2 \\
&\leq \|G_h(\bar{u}_h - \mathcal{I}_h u)\|^2 + C h^{2(k+1)} |u|_{k+2}^2 \\
&\leq |||u_h - \mathcal{I}_h u|||^2 + C h^{2(k+1)} |u|_{k+2}^2 \\
&\leq C h^{2\left(\min\left\{k+1, k+\frac{\alpha-1}{2}\right\}\right)} \|u\|_{k+2}^2,
\end{aligned}$$

which completes the proof. ∎

Remark 6.1 The estimate (6.7) shows that the gradient recovery $G_h u_h$ is superconvergent to ∇u when $\alpha \geq 1$. As the value of α increases, the convergence rate will also increase, and it reach the maximum rate of convergence $k+1$ when $\alpha = 3$.

7 | NUMERICAL EXPERIMENTS

In this section, we present some numerical examples to demonstrate the convergence of WG methods and the PPR recovery. We test our algorithm for the Q_1 and Q_2 elements, and choose different stabilizing parameters in our numerical algorithms for comparison. We focus on $|||u_h - \mathcal{I}_h u|||$, the error between the WG solution and its Lagrange interpolation in the energy norm, and $\|G_h u_h - \nabla u\|$, the error between the PPR recovered gradient and the true gradient in the L^2 norm.

Example 7.1 (Convergence for $k = 1$ on uniform meshes) In this example, we consider the problem (2.1) in the unit square $(0,1) \times (0,1)$, and use a family of uniform Cartesian meshes. The weak Galerkin space is given by

$$V_h = \{v = \{v_0, v_b\} : v_0|_T \in Q_1(T), v_b|_e \in P_1(e), e \subset \partial T, T \in \mathcal{T}_h\}. \tag{7.1}$$

The discrete weak gradient $\nabla_w v$ on each element $T \in \mathcal{T}_h$ is defined as

$$(\nabla_w v, \mathbf{q})_T = -(v_0, \nabla \cdot \mathbf{q})_T + \langle v_b, \mathbf{q} \cdot \mathbf{n} \rangle_{\partial T}, \quad \forall \mathbf{q} \in [Q_{0,1}, Q_{1,0}]^t. \tag{7.2}$$

The right-hand side function f is chosen such that the exact solution is

$$u = \sin(\pi x) \sin(\pi y). \tag{7.3}$$

Tables 1 and 2 report the convergence rates of $|||u_h - \mathcal{I}_h u|||$ and $\|G_h u_h - \nabla u\|$, respectively. Different values of the stabilizing parameter α have been tested. Here, the parameter

TABLE 1 Example 7.1. convergence of $|||u_h - \mathcal{I}_h u|||$ for $k = 1$ on uniform meshes.

	$\alpha = 1$		$\alpha = 2$		$\alpha = 3$	
N	$\|\|\|u_h - \mathcal{I}_h u\|\|\|$	Order	$\|\|\|u_h - \mathcal{I}_h u\|\|\|$	Order	$\|\|\|u_h - \mathcal{I}_h u\|\|\|$	Order
8	7.3081 e −01	–	3.0840 e −01	–	1.3216 e −01	–
16	3.6645 e −01	0.9959	1.0916 e −01	1.4983	3.3156 e −02	1.9949
32	1.8335 e −01	0.9990	3.8584 e −02	1.5004	8.2964 e −03	1.9987
64	9.1690 e −02	0.9998	1.3637 e −02	1.5005	2.0746 e −03	1.9997
128	4.5847 e −02	0.9999	4.8204 e −03	1.5003	5.1867 e −04	1.9999

TABLE 2 Example 7.1. convergence of $\|G_h u_h - \nabla u\|$ for $k = 1$ on uniform meshes.

	$\alpha = 1$		$\alpha = 2$		$\alpha = 3$	
N	$\|G_h u_h - \nabla u\|$	Order	$\|G_h u_h - \nabla u\|$	Order	$\|G_h u_h - \nabla u\|$	Order
8	1.0250 e −01	–	1.4942 e −01	–	1.5950 e −01	–
16	2.1339 e −02	2.2641	4.2838 e −02	1.8024	4.4857 e −02	1.8302
32	5.1285 e −03	2.0569	1.1614 e −02	1.8831	1.1909 e −02	1.9133
64	1.2692 e −03	2.0146	3.0197 e −03	1.9433	3.0591 e −03	1.9608
128	3.1624 e −04	2.0049	7.6942 e −04	1.9726	7.7448 e −04	1.9818

$N = 1/h$ denotes the number of rectangles in each direction. Table 1 clearly demonstrates that the convergence rate is $\min\{k+1, k+\frac{\alpha-1}{2}\}$, which is consistent with the error estimates (4.1). Table 2 indicates the superconvergence behavior of the PPR recovery. We note that for $\alpha = 1, 2$, the numerical results seem to be even better than our theoretical analysis (6.7).

Example 7.2 (Convergence for $k = 1$ on heterogeneous meshes) In this example, we investigate the superconvergence behavior on heterogeneous rectangular meshes. We use the same function (7.3) in this test. The initial mesh is randomly perturbed from the uniform mesh, and is given in Figure 5. The subsequent meshes are produced by uniform refinement. Errors are reported in Tables 3 and 4, in which similar superconvergence phenomenon is observed on these quasi-uniform rectangular meshes. Although the convergence rate of PPR recovered gradient for $\alpha = 1$ is not as high as in the uniform mesh in Example 7.1, but it is still higher than the analytical result (6.7).

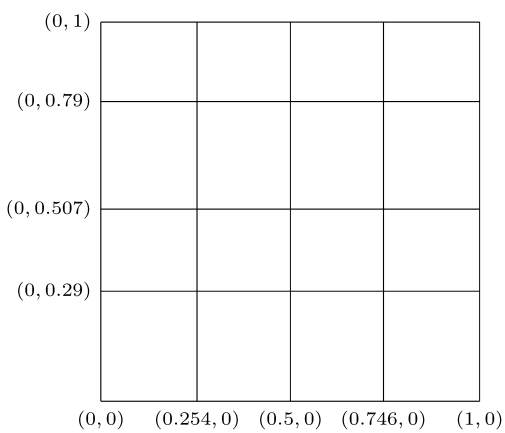

FIGURE 5 The initial partition

TABLE 3 Example 7.2. convergence of $|||u_h - \mathcal{I}_h u|||$ for $k = 1$ on heterogeneous meshes.

	$\alpha = 1$		$\alpha = 2$		$\alpha = 3$	
N	$\|\|\|u_h - \mathcal{I}_h u\|\|\|$	Order	$\|\|\|u_h - \mathcal{I}_h u\|\|\|$	Order	$\|\|\|u_h - \mathcal{I}_h u\|\|\|$	Order
8	7.3711 e −01	–	3.1389 e −01	–	1.3595 e −01	–
16	3.6979 e −01	0.9952	1.1114 e −01	1.4979	3.4117 e −02	1.9945
32	1.8504 e −01	0.9988	3.9284 e −02	1.5003	8.5374 e −03	1.9986
64	9.2540 e −02	0.9997	1.3885 e −02	1.5005	2.1349 e −03	1.9997
128	4.6272 e −02	0.9999	4.9079 e −03	1.5003	5.3375 e −04	1.9999

TABLE 4 Example 7.2. convergence of $\|G_h u_h - \nabla u\|$ for $k = 1$ on heterogeneous meshes.

	$\alpha = 1$		$\alpha = 2$		$\alpha = 3$	
N	$\|G_h u_h - \nabla u\|$	Order	$\|G_h u_h - \nabla u\|$	Order	$\|G_h u_h - \nabla u\|$	Order
8	1.1753 e −01	–	1.5431 e −01	–	1.6310 e −01	–
16	2.8433 e −02	2.0474	4.4400 e −02	1.7972	4.6371 e −02	1.8145
32	8.2896 e −03	1.7782	1.2080 e −02	1.8779	1.2381 e −02	1.9051
64	2.6255 e −03	1.6587	3.1488 e −03	1.9398	3.1897 e −03	1.9566
128	8.7219 e −04	1.5899	8.0340 e −04	1.9706	8.0870 e −04	1.9797

Example 7.3 (Convergence for $k = 2$) In this example, we test the superconvergence properties for some higher order WG approximations. In particular, we choose $k = 2$. Tables 5 and 6 list errors and the convergence rates for $u_h - \mathcal{I}_h u$ and $G_h u_h - \nabla u$, respectively.

Data in Tables 6 demonstrate that the PPR gradient recovery is superconvergent to ∇u. Numerical experiments for all three choices of α are of higher order convergence than our theoretical results. This surprising observation somehow indicates that there might be a more subtle relationship between the PPR recovery for WG solution and exact solution.

TABLE 5 Example 7.3. convergence of $|||u_h - \mathcal{I}_h u|||$ for $k = 2$ on uniform meshes.

	$\alpha = 1$		$\alpha = 2$		$\alpha = 3$	
N	$\|\|\|u_h - \mathcal{I}_h u\|\|\|$	Order	$\|\|\|u_h - \mathcal{I}_h u\|\|\|$	Order	$\|\|\|u_h - \mathcal{I}_h u\|\|\|$	Order
8	4.7148 e −02	–	2.0112 e −02	–	8.4797 e −03	–
16	1.1947 e −02	1.9805	3.5666 e −03	2.4954	1.0609 e −03	2.9987
32	2.9972 e −03	1.9950	6.3078 e −04	2.4994	1.3263 e −04	2.9998
64	7.4996 e −04	1.9987	1.1151 e −04	2.4999	1.6580 e −05	3.0000
128	1.8753 e −04	1.9997	1.9713 e −05	2.5000	2.0725 e −06	3.0000

TABLE 6 Example 7.3. convergence of $\|G_h u_h - \nabla u\|$ for $k = 2$ on uniform meshes.

	$\alpha = 1$		$\alpha = 2$		$\alpha = 3$	
N	$\|G_h u_h - \nabla u\|$	Order	$\|G_h u_h - \nabla u\|$	Order	$\|G_h u_h - \nabla u\|$	Order
8	4.4523 e −02	–	1.4339 e −02	–	1.0521 e −02	–
16	7.4403 e −03	2.5811	1.2958 e −03	3.4680	9.8726 e −04	3.4137
32	1.2791 e −03	2.5402	1.0979 e −04	3.5610	8.6269 e −05	3.5165
64	2.2415 e −04	2.5126	9.4297 e −06	3.5414	7.6241 e −06	3.5002
128	3.9531 e −05	2.5034	8.3447 e −07	3.4983	6.9244 e −07	3.4608

TABLE 7 Example 7.4. convergence of $|||u_h - \mathcal{I}_h u|||$ for $k = 1$ on uniform meshes.

$1/h$	$\alpha = 1$		$\alpha = 2$		$\alpha = 3$	
	$\|\|\|u_h - \mathcal{I}_h u\|\|\|$	Order	$\|\|\|u_h - \mathcal{I}_h u\|\|\|$	Order	$\|\|\|u_h - \mathcal{I}_h u\|\|\|$	Order
8	8.1780 e −02	–	3.5022 e −02	–	1.4989 e −02	–
16	4.1405 e −02	0.9820	1.2408 e −02	1.4970	3.7598 e −03	1.9952
32	2.0794 e −02	0.9936	4.3854 e −03	1.5005	9.4322 e −04	1.9950
64	1.0412 e −02	0.9979	1.5498 e −03	1.5006	2.3720 e −04	1.9915
128	5.2084 e −03	0.9994	5.4783 e −04	1.5003	5.9954 e −05	1.9842

As for now, (6.7) is the best theoretical estimate we can achieve. Improving the theoretical estimate will be an interesting future research project.

Example 7.4 (Convergence for less smooth functions) In this example, we consider the problem $-\Delta u = 1$, on the unit square with the homogeneous Dirichlet boundary condition. The exact solution can be written as

$$\begin{aligned} u(x,y) = \frac{x(1-x)+y(1-y)}{4} - \frac{2}{\pi^3}\sum_{i=0}^{\infty}\frac{1}{(2i+1)^3(1+\mathrm{e}^{-(2i+1)\pi})} \\ \cdot [(\mathrm{e}^{-(2i+1)\pi y} + \mathrm{e}^{-(2i+1)\pi(1-y)})\sin(2i+1)\pi x \\ + (\mathrm{e}^{-(2i+1)\pi x} + \mathrm{e}^{-(2i+1)\pi(1-x)})\sin(2i+1)\pi y]. \end{aligned} \tag{7.4}$$

The solution (7.4) is not as smooth as functions in previous examples. In fact, the function is in $H^{3-\epsilon}(\Omega)$ for any $\epsilon > 0$, but not in $H^3(\Omega)$, and it has a weak singularity $r^2 \ln r$ at the four corners of the domain. It is well-known that the nonsmoothness can affect the convergence and superconvergence of numerical schemes (see [18, 19]).

In the numerical test below, we truncate first fifty terms of the infinite sum as an approximation of the exact solution. We test both $k = 1$ and $k = 2$ cases on uniform meshes. Tables 7 and 8 report the convergence for $|||u_h - \mathcal{I}_h u|||$ and $\|G_h u_h - \nabla u\|$ for $k = 1$. Tables 9 and 10 report the convergence for $k = 2$.

We note that for $k = 1$, our superconvergence analysis requires the exact solution to be in H^3. Data in Tables 7 8 demonstrate that the convergence orders perfectly match or are even better than orders in our theoretical analysis. For higher order approximation $k = 2$, to get the analytical superconvergence order, we need the exact solution to be in H^4. However, the exact solution here is barely in H^3. Hence, some superconvergence behavior does not exist, which is reflected in Tables 9–10.

TABLE 8 Example 7.4. convergence of $\|G_h u_h - \nabla u\|$ for $k = 1$ on uniform meshes.

$1/h$	$\alpha = 1$		$\alpha = 2$		$\alpha = 3$	
	$\|G_h u_h - \nabla u\|$	Order	$\|G_h u_h - \nabla u\|$	Order	$\|G_h u_h - \nabla u\|$	Order
8	1.5971 e −02	–	1.0089 e −02	–	9.1308 e −03	–
16	4.6605 e −03	1.7769	2.4973 e −03	2.0157	2.3884 e −03	1.9347
32	1.4394 e −03	1.6950	6.4013 e −04	1.9639	6.2871 e −04	1.9526
64	4.7289 e −04	1.6059	1.6594 e −04	1.9477	1.6476 e −04	1.9320
128	1.6182 e −04	1.5471	4.3901 e −05	1.9183	4.3783 e −05	1.9120

TABLE 9 Example 7.4. convergence of $|||u_h - \mathcal{I}_h u|||$ for $k = 2$ on uniform meshes.

$1/h$	$\alpha = 1$		$\alpha = 2$		$\alpha = 3$	
	$\|\|\|u_h - \mathcal{I}_h u\|\|\|$	Order	$\|\|\|u_h - \mathcal{I}_h u\|\|\|$	Order	$\|\|\|u_h - \mathcal{I}_h u\|\|\|$	Order
8	5.0628 e −03	–	2.3506 e −03	–	1.0261 e −03	–
16	1.4579 e −04	1.7961	4.7629 e −04	2.3031	1.4729 e −04	2.8004
32	4.0745 e −04	1.8392	9.3998 e −05	2.3411	2.3929 e −05	2.6219
64	1.1214 e −04	1.8613	1.9466 e −05	2.2717	7.9370 e −06	1.5921
128	2.9974 e −05	1.9035	3.6114 e −06	2.4303	1.4716 e −06	2.4313

TABLE 10 Example 7.4. convergence of $\|G_h u_h - \nabla u\|$ for $k = 2$ on uniform meshes.

$1/h$	$\alpha = 1$		$\alpha = 2$		$\alpha = 3$	
	$\|G_h u_h - \nabla u\|$	order	$\|G_h u_h - \nabla u\|$	order	$\|G_h u_h - \nabla u\|$	order
8	5.8500 e −03	–	2.4904 e −03	–	2.1339 e −03	–
16	1.5089 e −03	1.9549	5.7978 e −04	2.1028	5.4716 e −04	1.9807
32	3.8325 e −04	1.9771	1.4062 e −04	2.0437	1.3706 e −04	1.9905
64	9.7663 e −05	1.9724	3.5701 e −05	1.9777	3.5286 e −05	1.9550
128	2.3997 e −05	2.0250	8.3963 e −06	2.0881	8.3497 e −06	2.0789

Remark 7.1 The condition regarding α is sharp in the supercloseness result (4.1). As we can see from data in Tables 1, 3, 5, and 7, the convergent rate follows loyally to the predicted $k + (\alpha - 1)/2$. Conversely, the condition regarding α may not be necessary for our superconvergence result in Theorem 6.4 as we can see from data in Tables 2, 4, 6, and 8: when $\alpha = 1, 2$, the supercloseness lost but the superconvergence still exists, since the supercloseness result (4.1) is a sufficient condition for Theorem 6.4, not a necessary condition.

8 | CONCLUSION

In this article, we analyze supercloseness of a class of WG methods for the elliptic equation. This supercloseness behavior is analyzed through newly designed stabilization terms. Superconvergence of the WG solution is obtained by a postprocessing using polynomial preserving recovery. Although these theoretical results are obtained for the Poisson equation on rectangular meshes, the numerical method itself can be readily applied to a wide variety of equations and triangular meshes.

ORCID

Xu Zhang http://orcid.org/0000-0003-4179-9552

REFERENCES

[1] J. Wang, X. Ye, *A weak Galerkin finite element method for second-order elliptic problems*, J. Comput. Appl. Math. vol. 241 (2013) pp. 103–115.

[2] L. Mu, J. Wang, X. Ye, *Weak Galerkin finite element methods on polytopal meshes*, Int. J. Numer. Anal. Model. vol. 12 (2015) pp. 31–53.

[3] J. Wang, X. Ye, *A weak Galerkin mixed finite element method for second order elliptic problems*, Math. Comp. vol. 83 (2014) pp. 2101–2126.

[4] L. Mu, J. Wang, X. Ye, S. Zhang, *A C0-weak Galerkin finite element method for the biharmonic equation*, J. Sci. Comput. vol. 59 (2014) pp. 473–495.

[5] R. Zhang, Q. Zhai, *A weak Galerkin finite element scheme for the biharmonic equations by using polynomials of reduced order*, J. Sci. Comput. vol. 64 (2015) pp. 559–585.

[6] D. N. Arnold, J. Douglas, V. Thomée, *Superconvergence of a finite element approximation to the solution of a Sobolev equation in a single space variable*, Math. Comp. vol. 36 (1981) pp. 53–63.

[7] I. Babuška, T. Strouboulis, *The finite element method and its reliability*, Numer. Math. Sci. Comput., Clarendon, New York, 2001.

[8] J. Douglas, A superconvergence result for the approximate solution of the heat equation by a collocation method, The Mathematical Foundations of the Finite Element Method with Applications to Partial Differential Equations, Academic Press, New York, 1972, pp. 475–490.

[9] Y. Huang, J. Li, Q. Lin, *Superconvergence analysis for time-dependent Maxwell's equations in metamaterials*, Numer. Methods Partial Differential Equations, vol. 28 (2012) pp. 1794–1816.

[10] M. Křížek, P. Neittaanmäki, R. Stenberg, eds., Finite element methods: superconvergence, post-processing, and a posteriori estimates, Lecture Notes in Pure and Appl. Math. vol. 196, Marcel Dekker, New York, 1997.

[11] A. H. Schatz, I. H. Sloan, L. B. Wahlbin, *Superconvergence in finite element methods and meshes that are locally symmetric with respect to a point*, SIAM J. Numer. Anal. vol. 33 (1996) pp. 505–521.

[12] L. B. Wahlbin, Superconvergence in Galerkin Finite Element Methods, Lecture Notes in Math. 1605, Springer, Berlin, 1995.

[13] A. Naga, Z. Zhang, *A posteriori error estimates based on the polynomial preserving recovery*, SIAM J. Numer. Anal. vol. 42 (2004) pp. 1780–1800.

[14] A. Naga, Z. Zhang, *The polynomial-preserving recovery for higher order finite element methods in 2D and 3D*, Discrete Contin. Dyn. Syst. Ser. B vol. 5 (2005) pp. 769–798.

[15] Z. Zhang, A. Naga, *A new finite element gradient recovery method: superconvergence property*, SIAM J. Sci. Comput. vol. 26 (2005) pp. 1192–1213.

[16] A. Harris, S. Harris, *Superconvergence of weak Galerkin finite element approximation for second order elliptic problems by L2-projections*, Appl. Math. Comput. vol. 227 (2014), pp. 610–621.

[17] T. Zhang, S. Yu, *The derivative patch interpolation recovery technique and superconvergence for the discontinuous Galerkin method*, Appl. Numer. Math. vol. 85 (2014) pp. 128–141.

[18] P. Grisvard, Elliptic problems in nonsmooth domains, Monographs and Studies in Mathematic 24, Pitman, Boston, MA, 1985.

[19] V. A. Kondratév, *Boundary value problems for elliptic equations in domains with conical or angular points*, Trudy Moskov. Mat. Obsc. vol. 16 (1967) pp. 209–292.

How to cite this article: Wang R, Zhang R, Zhang X, Zhang Z. Supercloseness analysis and polynomial preserving Recovery for a class of weak Galerkin Methods. *Numer Methods Partial Differential Eq*. 2018;34:317–335. https://doi.org/10.1002/num.22201